NOLTA, IEICE

Paper

Enhancement of noise correlation for noise-induced synchronization of limit-cycle oscillators by threshold filtering

Masahiro Kazama [1], *Wataru Kurebayashi* [2a)], *Takahiro Tsuchida* [2], *Yuta Minoshima* [2], *Mikio Hasegawa* [3], *Koji Kimura* [2], *and Hiroya Nakao* [2]

[1] *Graduate School of Interdisciplinary Information Studies, The University of Tokyo, 7-3-1 Hongo, Bunkyo-ku, Tokyo 113-0033, Japan*

[2] *Graduate School of Information Science and Engineering, Tokyo Institute of Technology, 2-12-1 O-okayama, Meguro-ku, Tokyo 152-8552, Japan*

[3] *Department of Electrical Engineering, Tokyo University of Science, 6-3-1 Niijuku, Katsushika-ku, Tokyo 125-8585, Japan*

[a)] *kurebayashi.w.aa@m.titech.ac.jp*

Received July 10, 2013; Revised November 21, 2013; Published April 1, 2014

Abstract: Nonlinear oscillators driven by correlated noisy signals can synchronize without direct mutual interactions. Here we show that correlation between noisy signals can be enhanced by applying a threshold filter, and the filtered signals can be used to improve noise-induced synchronization. We derive analytical expressions for the correlation coefficient between the filtered signals, and, using simple examples, we demonstrate that the correlation can actually be enhanced and the synchronization can be improved by the threshold filtering in some cases.

Key Words: nonlinear oscillators, noise-induced synchronization, threshold filtering, signal processing, noise correlation

1. Introduction

When nonlinear oscillators are driven by common or correlated noisy signals, they can mutually synchronize even in the absence of periodic driving signals or direct mutual interactions. This phenomenon, called the noise-induced synchronization or stochastic synchronization, has widely been observed in various experimental systems, e.g., in spiking neurons, electric circuits, and lasers [1–3]. Synchronous behavior of certain neurophysiological systems, such as olfactory bulb neurons and spinal motor neurons [4, 5], and that of certain ecological systems, such as synchronized masting of plants and synchronous variations of ecological populations [6], are also considered to be caused

Nonlinear Theory and Its Applications, IEICE, vol. 5, no. 2, pp. 157–171 DOI: 10.1588/nolta.5.157

by correlated biological or environmental fluctuations. Engineering applications of the mechanism of noise-induced synchronization for high-speed integrated circuits and communication systems have also been attempted recently [7, 8]. See Fig. 1 for a numerical illustration of the noise-induced synchronization between two phase oscillators driven by correlated noisy signals measured by acceleration sensors on a train.

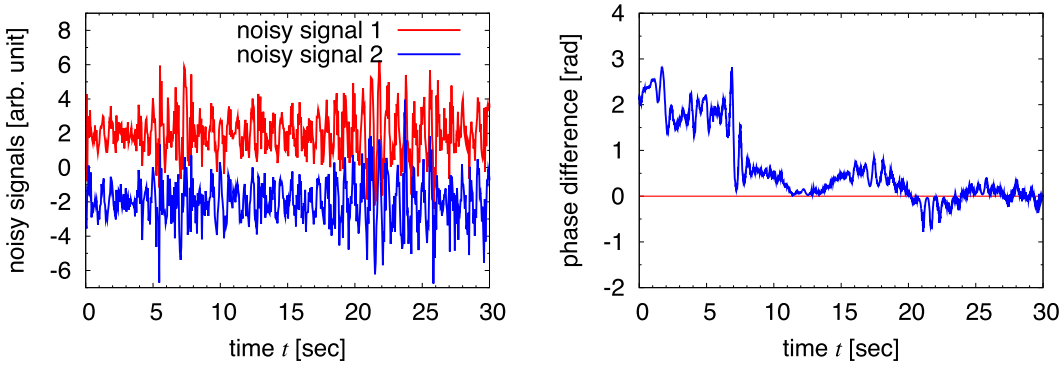

(a) Noisy signals (b) Phase difference

Fig. 1. Noise-induced synchronization of nonlinear oscillators driven by correlated noisy signals measured by acceleration sensors of two iPads placed nearby on the shelf of a train running along the Japan Railway Yamanote loop in Tokyo. The data are sampled with an interval of 10 milliseconds during one cycle of the train around the loop (about 35 kilometers, 3636 seconds). The measured noisy signals are appropriately normalized and used to drive a pair of phase oscillators described by Eq. (17) with $\omega = 0.6$ and $Z(\theta) = 5\sin\theta$. (a) Typical time series of the noisy signals. (b) Evolution of the phase difference.

Key studies on the noise-induced synchronization of limit-cycle oscillators were carried out by Teramae and Tanaka [9], and by Goldobin and Pikovsky [10], who analytically showed, by using the phase-reduction method [11], that two identical limit-cycle oscillators driven by common weak Gaussian-white noise always synchronize with each other, except for some special cases. Their results have later been extended to limit-cycle oscillators driven by non-white noise with general power spectra and probability densities [12]. Also, global characterization of the synchronization properties using stationary probability densities of the phase differences between the oscillators was performed on the basis of the effective Fokker-Planck equation [13, 14]. Generally, the degree of synchronization is improved as the noise correlation becomes stronger.

In real-world systems, however, two noisy signals can never be identical even if they are measured at spatially adjacent locations. Thus, if synchronization of some oscillatory systems are induced by noise, the quality of synchronization depends on the correlation between the noisy signals. Moreover, if some biological systems utilize environmental noise for synchronization, they may pre-process the incoming noise before driving their internal clocks to improve synchrony. It is thus interesting to consider how the correlation between two noisy signals can be enhanced for synchronization.

In this paper, we show that a simple threshold filter can enhance the correlation between two noisy signals and improve noise-induced synchronization in some situations. We derive an analytical expression for the correlation coefficient of two noisy signals transformed by the threshold filter, and use it to predict stationary distributions of the phase differences between two limit-cycle oscillators driven by the filtered noise.

2. Enhancement of noise correlation

Let us consider two noisy signals $s_1(t)$ and $s_2(t)$, which are correlated but not identical. We assume that $s_1(t)$ and $s_2(t)$ are mixtures of a common component $\xi(t)$ and two independent components of equal intensity $\eta_{1,2}(t)$ given by

$$\begin{aligned} s_1(t) &= \xi(t) + \eta_1(t), \\ s_2(t) &= \xi(t) + \eta_2(t). \end{aligned} \tag{1}$$

Here, $\xi(t)$ and $\eta_{1,2}(t)$ are assumed to be stationary, uncorrelated noisy signals of mean values μ_ξ, μ_η and variance σ_ξ^2, σ_η^2 as follows:

$$\mu_\xi = E[\xi(t)],\ \ \mu_\eta = E[\eta_{1,2}(t)],\ \ \sigma_\xi^2 = E[(\xi(t)-\mu_\xi)^2],\ \ \sigma_\eta^2 = E[(\eta_{1,2}(t)-\mu_\eta)^2], \tag{2}$$

$$E[(\xi(t)-\mu_\xi)(\eta_{1,2}(t)-\mu_\eta)] = E[(\eta_1(t)-\mu_\eta)(\eta_2(t)-\mu_\eta)] = 0. \tag{3}$$

We also assume that $\eta_1(t)$ and $\eta_2(t)$ obey the same probability distribution (see Appendix E for a discussion). As long as the correlation times of $\xi(t)$ and $\eta_{1,2}(t)$ are finite, autocorrelation functions of $\xi(t)$ and $\eta_{1,2}(t)$ can be chosen arbitrarily in the following argument.

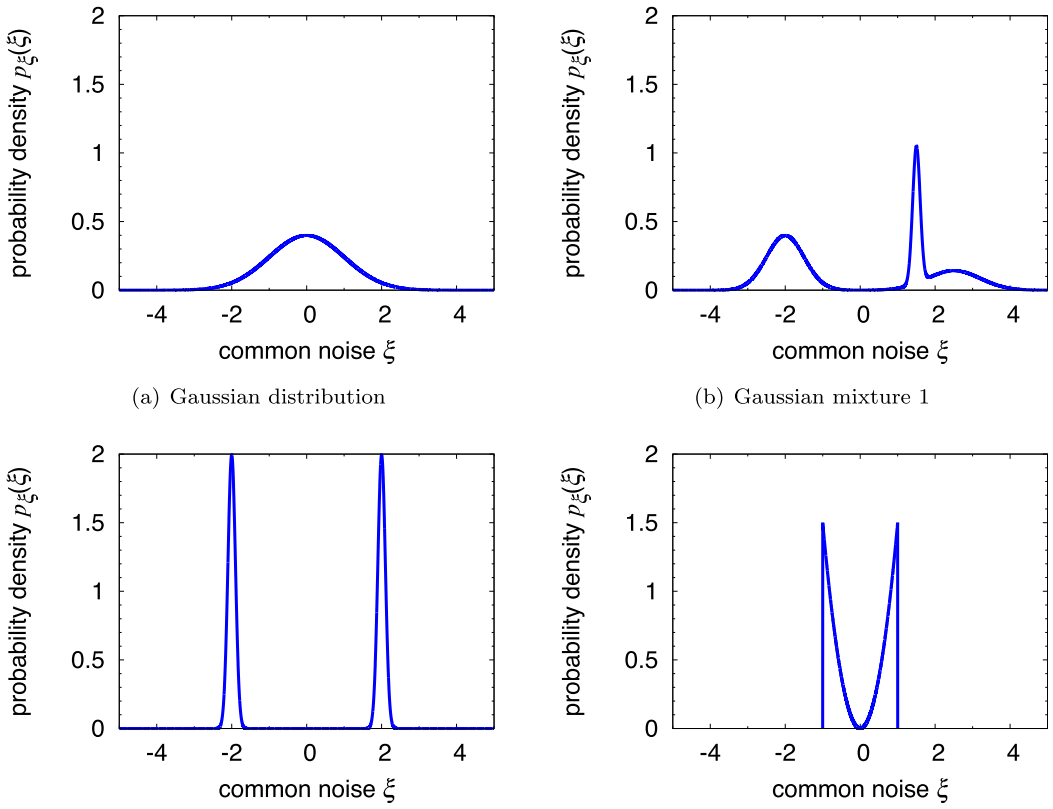

(a) Gaussian distribution (b) Gaussian mixture 1

(c) Gaussian mixture 2 (d) Quadratic bimodal distribution

Fig. 2. Probability density functions of the common noisy signals used as examples for the calculation of correlation coefficients.

To enhance the correlation between the noisy signals $s_1(t)$ and $s_2(t)$, we introduce a simple threshold filter $\Theta(s)$ and generate new noisy signals $\tilde{s}_1(t)$ and $\tilde{s}_2(t)$ as follows:

$$\tilde{s}_i(t) = \Theta(s_i(t)) = \begin{cases} 1 & (s_i(t) \geq h), \\ -1 & (s_i(t) < h), \end{cases} \tag{4}$$

for $i = 1, 2$, where h represents the threshold value. The correlation coefficient ρ between the original raw signals $s_1(t)$ and $s_2(t)$ is defined as

$$\rho = \frac{E\left[\left(s_1(t) - E[s_1(t)]\right)\left(s_2(t) - E[s_2(t)]\right)\right]}{\sqrt{E\left[\left(s_1(t) - E[s_1(t)]\right)^2\right]}\sqrt{E\left[\left(s_2(t) - E[s_2(t)]\right)^2\right]}} \tag{5}$$

and can explicitly be calculated as

$$\rho = \frac{\sigma_\xi^2}{\sigma_\xi^2 + \sigma_\eta^2}. \tag{6}$$

Similarly, the correlation coefficient $\tilde{\rho}$ between the filtered signals $\tilde{s}_1(t)$ and $\tilde{s}_2(t)$ is defined as

$$\tilde{\rho} = \frac{E\big[\big(\tilde{s}_1(t) - E[\tilde{s}_1(t)]\big)\big(\tilde{s}_2(t) - E[\tilde{s}_2(t)]\big)\big]}{\sqrt{E\big[\big(\tilde{s}_1(t) - E[\tilde{s}_1(t)]\big)^2\big]}\sqrt{E\big[\big(\tilde{s}_2(t) - E[\tilde{s}_2(t)]\big)^2\big]}}. \tag{7}$$

Denoting the probability density function (PDF) of the common noise $\xi(t)$ as $p_\xi(\xi)$, the PDF of the independent noise $\eta_{1,2}(t)$ as $p_\eta(\eta_{1,2})$, and the cumulative density function (CDF) of the independent noise $\eta_{1,2}(t)$ as $\Phi_\eta(\eta) = \int_{-\infty}^{\eta} p_\eta(\eta')d\eta'$, respectively, we can explicitly calculate $\tilde{\rho}$ as (see Appendix A for the derivation)

$$\tilde{\rho} = \frac{\int_{-\infty}^{+\infty} \Phi_\eta^2(u-h)p_\xi(u)du - \big\{\int_{-\infty}^{+\infty} \Phi_\eta(u-h)p_\xi(u)du\big\}^2}{\int_{-\infty}^{+\infty} \Phi_\eta(u-h)p_\xi(u)du - \big\{\int_{-\infty}^{+\infty} \Phi_\eta(u-h)p_\xi(u)du\big\}^2}. \tag{8}$$

Thus, $\tilde{\rho}$ is determined from the PDF p_ξ of the common noise and the CDF Φ_η of the independent noise, and depends on the threshold value h.

Without loss of generality, we can assume that the independent noise is zero-mean ($\mu_\eta = 0$). Then, we can obtain the following approximation of the filtered correlation coefficient, which is valid when the independent noise is sufficiently weaker than the common noise (see Appendix B for the derivation):

$$\tilde{\rho} = 1 - \frac{p_\xi(h)\int_{-\infty}^{\infty} \Phi_\eta(u)\{1-\Phi_\eta(u)\}du}{\Phi_\xi(h)(1-\Phi_\xi(h))} + O\left(\Phi_\xi''(h)\sigma_\eta^2\right). \tag{9}$$

Moreover, if the independent noise is Gaussian, we can express $\tilde{\rho}$ as

$$\tilde{\rho} = 1 - \frac{\sigma_\eta p_\xi(h)}{\sqrt{\pi}\Phi_\xi(h)(1-\Phi_\xi(h))} + O\left(\Phi_\xi''(h)\sigma_\eta^2\right). \tag{10}$$

These approximate expressions can be used in choosing the appropriate threshold value h.

As examples, we consider the following 4 types of PDFs (a Gaussian distribution, two types of Gaussian mixtures, and a quadratic bimodal distribution) shown in Fig. 2:

$$p_\xi^{(1)}(\xi) = \mathcal{G}(\xi; 0, 1), \tag{11}$$

$$p_\xi^{(2)}(\xi) = 0.5\mathcal{G}(\xi; -2, 0.5) + 0.25\mathcal{G}(\xi; 1.5, 0.1) + 0.25\mathcal{G}(\xi; 2.5, 0.7), \tag{12}$$

$$p_\xi^{(3)}(\xi) = 0.5\mathcal{G}(\xi; -2, 0.1) + 0.5\mathcal{G}(\xi; 2, 0.1), \tag{13}$$

$$p_\xi^{(4)}(\xi) = \frac{3x^2}{2} \ \ (-1 < x < 1) \ \text{ and } \ 0 \ \text{ (otherwise)}, \tag{14}$$

where

$$\mathcal{G}(u; a, b) = \frac{1}{\sqrt{2\pi}b}\exp\left[-\frac{(u-a)^2}{2b^2}\right] \tag{15}$$

represents a Gaussian distribution of mean a and standard deviation b. The independent noise is also assumed to be Gaussian-distributed with mean 0 and standard deviation σ_η as

$$p_\eta(\eta) = \mathcal{G}(\eta; 0, \sigma_\eta). \tag{16}$$

Figure 3 shows the correlation coefficients ρ and $\tilde{\rho}$ of the raw and filtered noisy signals obeying the above 4 types of the probability distributions. The standard deviation of the independent noise is fixed at $\sigma_\eta = 0.2$, and ρ, $\tilde{\rho}$ are plotted as functions of the threshold value h. For the Gaussian distribution, no enhancement in correlation occurs by the application of the threshold filter (Figs. 3(a,b)); the filtered correlation $\tilde{\rho}$ is always smaller than the raw correlation ρ (see Appendix D for a discussion). For the two types of Gaussian mixtures, the threshold filter slightly increases the correlation ($\tilde{\rho} > \rho$) in a range of the threshold value h (Figs. 3(c,d) and (e,f)). For the quadratic bimodal distribution, the

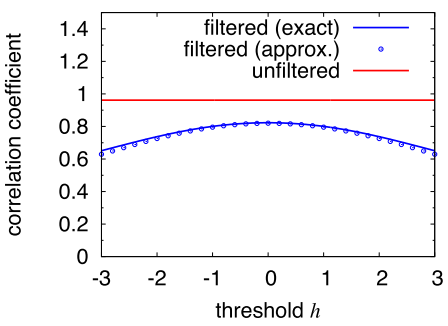

(a) Gaussian distribution

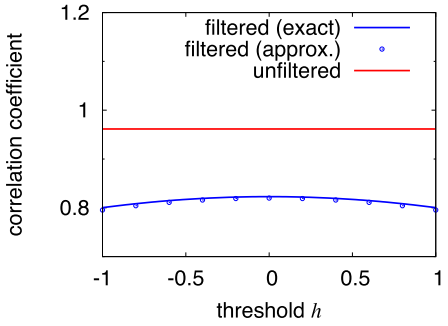

(b) Gaussian distribution (enlarged)

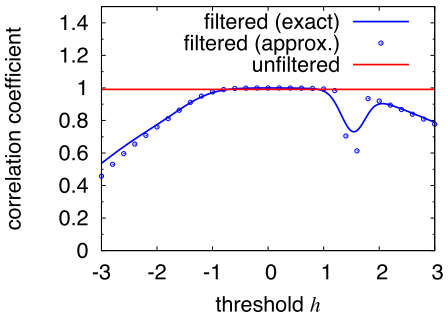

(c) Gaussian mixture 1

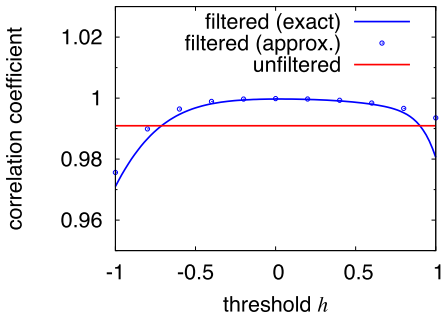

(d) Gaussian mixture 1 (enlarged)

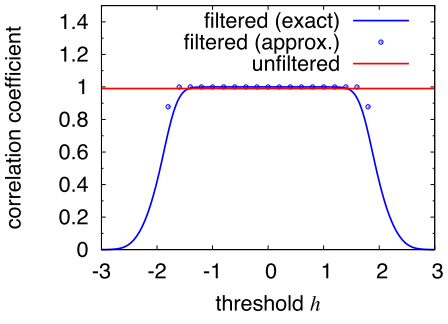

(e) Gaussian mixture 2

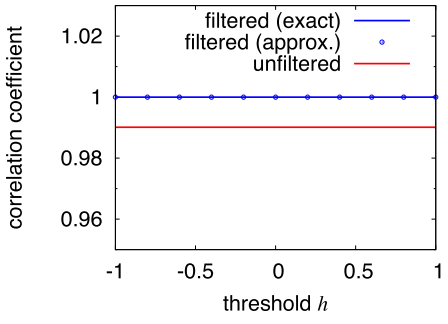

(f) Gaussian mixture 2 (enlarged)

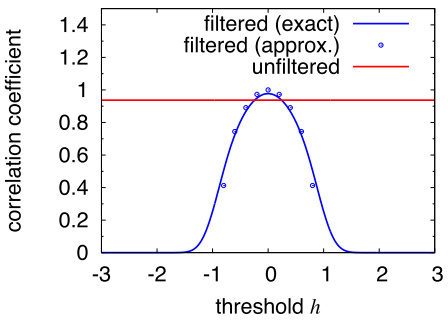

(g) Quadratic bimodal distribution

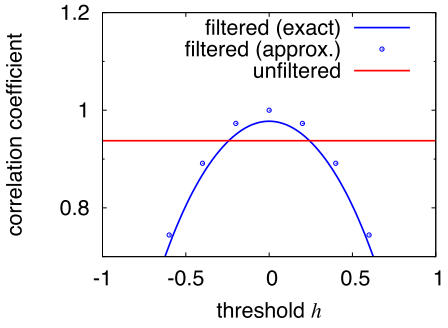

(h) Quadratic bimodal distribution (enlarged)

Fig. 3. Correlation coefficients ρ and $\tilde{\rho}$. The standard deviation of the independent noise is fixed at $\sigma_\eta = 0.2$, and the threshold value h is varied. The red lines show the correlation ρ of the raw signals, the blue curves show the correlation $\tilde{\rho}$ of the filtered signals, and blue dots show the approximation to $\tilde{\rho}$ for weak independent Gaussian noise.

correlation is visibly enhanced ($\tilde{\rho} > \rho$) by the threshold filter when $|h|$ is relatively small (Figs. 3(g,h)), and takes a maximum value at $h = 0$. As $|h|$ increases, the filtered correlation $\tilde{\rho}$ quickly decreases and becomes lower than the raw correlation ρ.

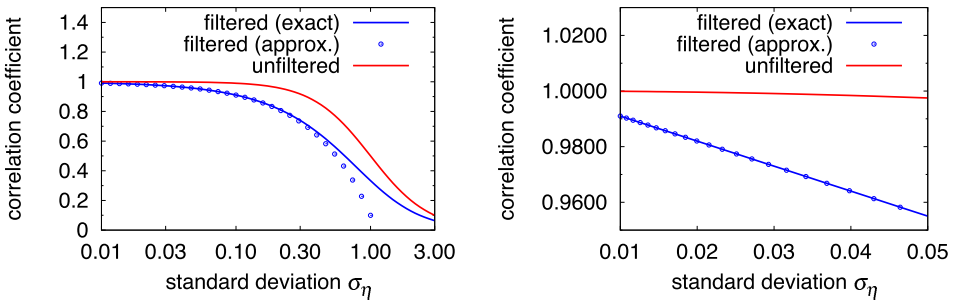

(a) Gaussian distribution (b) Gaussian distribution (enlarged)

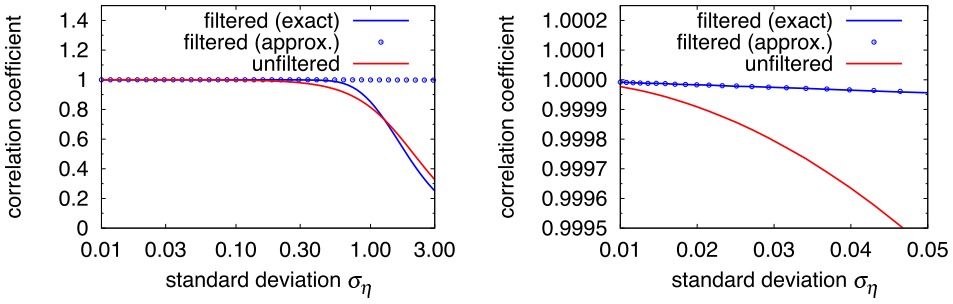

(c) Gaussian mixture 1 (d) Gaussian mixture 1 (enlarged)

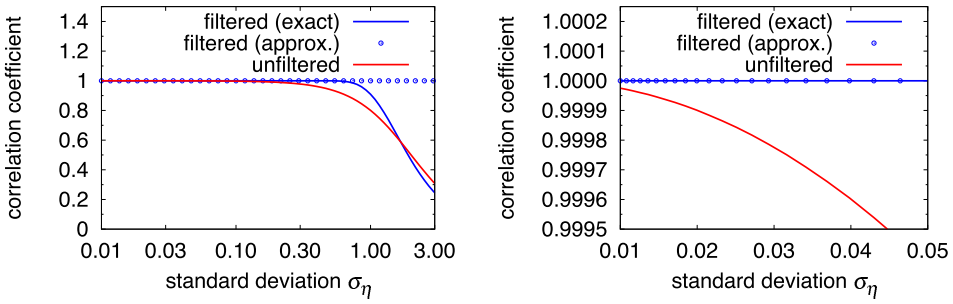

(e) Gaussian mixture 2 (f) Gaussian mixture 2 (enlarged)

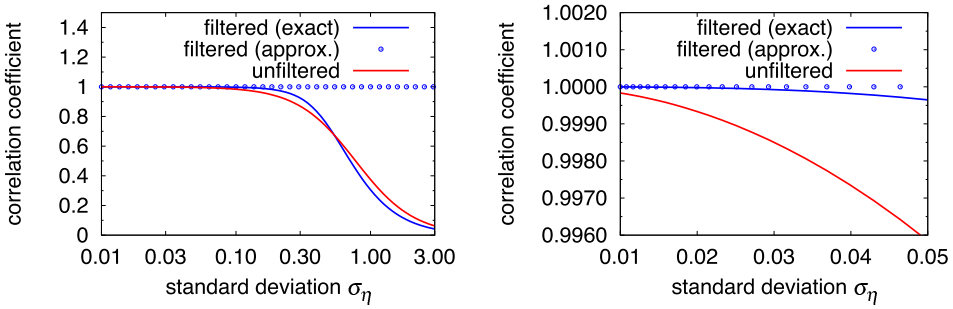

(g) Quadratic bimodal distribution (h) Quadratic bimodal distribution (enlarged)

Fig. 4. Correlation coefficients ρ and $\tilde{\rho}$. The threshold value is fixed at $h = 0$, and the standard deviation of the independent noise σ_η is varied. The red curves show the correlation ρ of the raw signals, the blue curves show the correlation $\tilde{\rho}$ of the filtered signals, and blue dots show the approximation to $\tilde{\rho}$ for weak independent Gaussian noise.

Figure 4 shows the correlation coefficients ρ and $\tilde{\rho}$ of the raw and filtered noisy signals as functions of the standard deviation of the independent noise σ_η, where the threshold value h is fixed at 0. Both the raw correlation ρ and filtered correlation $\tilde{\rho}$ are decreasing functions of σ_η. For the Gaussian

distribution, no enhancement in correlation is observed in the entire range of the standard deviation σ_η (Figs. 4(a,b)); the filtered correlation $\tilde{\rho}$ is always smaller than the raw correlation ρ ($\tilde{\rho} < \rho$). For the two types of Gaussian mixtures, the filtered correlation $\tilde{\rho}$ is larger than the raw correlation ρ when σ_η is smaller than a certain critical value (Figs. 4(c,d) and (e,f)). The enhancement of correlation increases with σ_η, and the maximum enhancement is attained around $\sigma_\eta \approx 1$. When σ_η is further increased, $\tilde{\rho}$ quickly decreases and becomes smaller than ρ. Similarly, for the quadratic bimodal distribution, the correlation is enhanced for σ_η between 0 and a certain critical value around 0.5 (Figs. 4(g,h)). As σ_η is increased further, the filtered correlation $\tilde{\rho}$ quickly decreases and becomes lower than the raw correlation ρ. The approximation formula for weak Gaussian independent noise is valid for relatively small σ_η, but the deviation becomes larger as σ_η is increased.

Thus, we have observed that the threshold filter can enhance the correlation between noisy signals in some cases, where the noisy signals have a common non-Gaussian component. In the next section, we use the filtered noisy signals for noise-induced synchronization of limit-cycle oscillators and show that the synchrony can be improved.

3. Noise-induced synchronization

We consider a pair of identical limit-cycle oscillators driven by weak correlated noisy signals, which can be described by the following phase Langevin equations [9, 12–14]:

$$\begin{aligned} \dot{\theta}_1(t) &= \omega + Z(\theta_1)s_1(t), \\ \dot{\theta}_2(t) &= \omega + Z(\theta_2)s_2(t), \end{aligned} \tag{17}$$

where $\theta_{1,2}$ are the phase variables of the oscillators, ω is a natural frequency of the oscillators, $Z(\theta)$ is a phase sensitivity function [11] quantifying the phase response of the oscillator to infinitesimal perturbations, and $s_{1,2}(t)$ are the mutually correlated noisy signals with correlation coefficient ρ given by Eq. (1). Under mild conditions, it can be shown that the phase difference $\psi = \theta_1 - \theta_2$ between the two oscillators shrinks to $\psi = 0$ on average and distributes around $\psi = 0$. Namely, the two oscillators tend to synchronize with each other statistically, though they are subject to occasional phase slips caused by the independent components of the noisy signals.

As shown in [14], synchrony between the oscillators may not always be improved even if the correlation coefficient ρ between the noisy signals is increased. However, using the results of [14], it can be shown that, when all $\xi(t)$, $\eta_1(t)$, $\eta_2(t)$ have the same power spectrum (or the same autocorrelation function), the stationary PDF $q(\psi)$ of the phase difference ψ can be expressed using the noise correlation ρ as

$$q(\psi) = \frac{N}{g(0) - \rho g(\psi)}, \tag{18}$$

where N is a normalization constant, and the function $g(\psi)$ is a function defined by

$$g(\psi) = \sum_{\ell=-\infty}^{+\infty} |Z_\ell|^2 P(\ell\omega) e^{i\ell\psi}, \tag{19}$$

where $Z_\ell \in \mathbb{C}$ is the ℓ-th Fourier coefficient of $Z(\theta)$ and $P(\Omega)$ is the power spectrum of $\xi(t)$ and $\eta_{1,2}(t)$. As shown in Fig. 5, the PDF $q(\psi)$ given by Eq. (18) generally has a peak at $\psi = 0$ when the correlation coefficient ρ is sufficiently large, indicating that the phase difference distributes around $\psi = 0$, i.e., the two oscillators are stochastically synchronized. Our interest is if the peak becomes more pronounced when the filtered noisy signals $\tilde{s}_{1,2}$ are used in place of the raw noisy signals $s_{1,2}$ in Eq. (17), which is expected to occur when $\tilde{\rho} > \rho$ from Eq. (18) (note that $0 \le \rho, \tilde{\rho} \le 1$).

We performed numerical simulations of the phase model (17) using the raw noisy signals $s_{1,2}$ and the filtered noisy signals $\tilde{s}_{1,2}$, where the common component $\xi(t)$ obeys either of the Gaussian mixture 2 and the quadratic bimodal distribution (see Appendix C for numerical generation of the noise). The autocorrelation function of each noise is given by

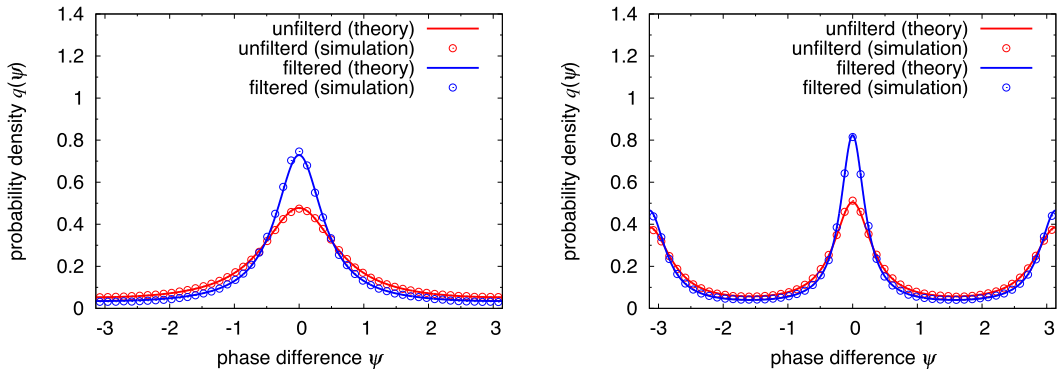

(a) Gaussian mixture 2, $Z^{(1)}(\theta)$ (b) Gaussian mixture 2, $Z^{(2)}(\theta)$

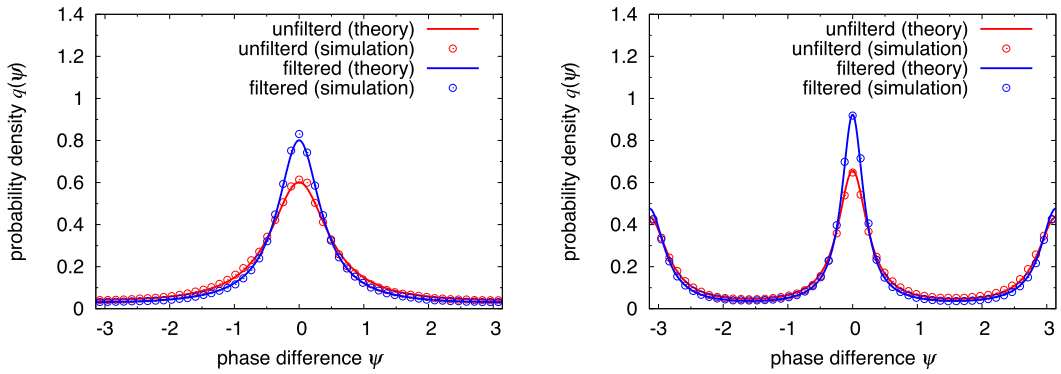

(c) Quadratic bimodal distribution, $Z^{(1)}(\theta)$ (d) Quadratic bimodal distribution, $Z^{(2)}(\theta)$

Fig. 5. Stationary probability density functions of the phase difference between two oscillators driven by correlated noisy signals. Solid curves show the results of the theory, and circles show the results of numerical simulations. Red curves are obtained for raw noisy signals without filtering, and blue curves show the results for filtered noisy signals. (a,b) Gaussian mixture 2 and $\sigma_\eta = 1$. (c,d) Quadratic bimodal distribution and $\sigma_\eta = 0.3$. (a,c) $Z^{(1)}(\theta)$. (b,d) $Z^{(2)}(\theta)$. The raw and filtered correlations ρ, $\tilde{\rho}$ between the noisy signals and the order parameters R_1, R_2 calculated from $q(\psi)$ are (a) $\rho = 0.80$, $\tilde{\rho} = 0.91$, $R_1 = 0.50$, $R_2 = 0.25$, $\tilde{R}_1 = 0.64$, $\tilde{R}_2 = 0.41$, (b) $\rho = 0.80$, $\tilde{\rho} = 0.91$, $R_1 = 0.07$, $R_2 = 0.47$, $\tilde{R}_1 = 0.14$, $\tilde{R}_2 = 0.60$, (c) $\rho = 0.87$, $\tilde{\rho} = 0.92$, $R_1 = 0.58$, $R_2 = 0.34$, $\tilde{R}_1 = 0.67$, $\tilde{R}_2 = 0.45$, (d) $\rho = 0.87$, $\tilde{\rho} = 0.92$, $R_1 = 0.10$, $R_2 = 0.55$, $\tilde{R}_1 = 0.16$, $\tilde{R}_2 = 0.62$.

$$C(t) = E\left[\left(f(k) - E[f(k)]\right)^2\right]\left(1 - \frac{|t|}{\delta t}\right) \quad (-\delta t < t < \delta t), \quad 0 \quad \text{(otherwise)}, \tag{20}$$

where $\delta t = 0.1$ and $f(k)$ $(k = 1, 2, 3, ..., N)$ is an uncorrelated noisy time sequence drawn independently from a given probability distribution. The corresponding power spectrum $P(\Omega)$ is given by

$$P(\Omega) = \int_{-\infty}^{\infty} C(t) e^{-i\Omega t} dt = E\left[\left(f(k) - E[f(k)]\right)^2\right] \frac{2 - 2\cos(\Omega \delta t)}{\Omega^2 \delta t}. \tag{21}$$

For each distribution of the common noise, numerical and theoretical results are plotted in Figs. 2(a,b) and Figs. 2(c,d), respectively. For each case, the independent noise is assumed to obey Gaussian distribution of standard deviation $\sigma_\eta = 1.0$ [Figs. 5(a,b)] and $\sigma_\eta = 0.3$ [Figs. 5(c,d)]. The natural frequency is fixed at $\omega = 1$, and the following two types of the phase sensitivity functions are used:

$$Z^{(1)}(\theta) = 0.1 \sin\theta, \tag{22}$$

$$Z^{(2)}(\theta) = 0.02 \sin\theta + 0.1 \sin 2\theta. \tag{23}$$

The threshold value h is chosen so that maximum enhancement in correlation is attained, i.e., $h = 0$ for both the Gaussian mixture 2 and the quadratic bimodal distribution, which are estimated from Fig. 3. In general, we can use the expression of $\tilde{\rho}$ given in Eqs. (8), (9), and (10) to find the optimal value of h when the PDFs $p_\xi(\xi)$ and $p_\eta(\eta_i)$ of the common and independent components are given.

As can be seen from Fig. 5, the distribution $q(\psi)$ of the phase difference has a higher and narrower peak when the filtered noisy signals $\tilde{s}_{1,2}$ are used in place of the raw noisy signals $s_{1,2}$. Thus, the application of the threshold filter to the raw noisy signals can actually improve synchrony of limit-cycle oscillators driven by correlated noise for the above two types of the noise distributions. The results of numerical simulations agree well with the theory [Eq. (18)].

To quantify the degree of synchronization, we calculate the order parameters

$$R_k = \left| \int_{-\pi}^{\pi} e^{ik\psi} q(\psi) d\psi \right| \quad (k = 1, 2) \tag{24}$$

from the stationary PDF $q(\psi)$ of the phase difference of the two oscillators driven by the noisy signals before and after threshold filtering (the filtered values are denoted as $\tilde{R}_1$, $\tilde{R}_2$). When the oscillators are completely desynchronized, $q(\psi) = (2\pi)^{-1}$, the order parameters take $R_1 = R_2 = 0$, and when the oscillators are completely synchronized, $q(\psi) = \delta(\psi)$, $R_1 = R_2 = 1$. The parameter R_2 also quantifies the secondary peaks at $\psi = \pm\pi$ of the distribution, i.e., noise-induced anti-phase synchronization of the oscillators caused by the second-order harmonic component in $Z(\theta)$, as shown in Figs. 5(b) and (d). The actual values of R_1 and R_2 calculated from the stationary PDF of the phase difference are shown in the caption of Fig. 5.

4. Summary

We showed that a simple threshold filter can enhance correlation between noisy signals and improve noise-induced synchronization between a pair of limit-cycle oscillators for several types of noise. We derived the correlation coefficient between the filtered noisy signals, and showed that the correlation can be enhanced for several types of noise distributions. We also observed that the threshold filter does not enhance the correlation but rather diminish it for the Gaussian noise. Actually, the correlation appears to be diminished for a large class of unimodal noise PDFs by the threshold filter, implying that the threshold filter may not be a good candidate for robust enhancement of noise correlation. Though we considered only the simplest threshold filter in this study, more general nonlinear filtering methods may produce more correlated noise appropriate for noise-induced synchronization.

Recently, synchronization of heterogeneous oscillators with different phase sensitivity functions driven by correlated noisy signals has been studied in [15]. It is reported that heterogeneous oscillator pairs can synchronize better than homogeneous pairs possessing the same phase sensitivity functions when the noise correlation is weak. Though the considered physical situations are different, this result can be relevant to our problem, as it suggests another possibility of improving synchronization induced by correlated noise. Incorporating the effect of oscillator heterogeneity into our problem setting should also be important for practical applications.

Acknowledgments

M. H. and H. N. thank K. Aihara and Y. Horio for useful discussions, and acknowledge the Aihara Project, the FIRST program from JSPS, initiated by CSTP for financial support. H. N. also thanks KAKENHI 22684020 (JSPS) and CREST Kokubu project (JST) for financial support.

Appendix

A. Derivation of Eq. (8)

Here, we derive the expression of $\tilde{\rho}$ in Eq. (8). From Eq. (7), $\tilde{\rho}$ can be written as follows:

$$\tilde{\rho} = \frac{E[\tilde{s}_1(t)\tilde{s}_2(t)] - E[\tilde{s}_1(t)]E[\tilde{s}_2(t)]}{E[\{\tilde{s}_{1,2}(t)\}^2] - E[\tilde{s}_{1,2}(t)]^2}, \tag{A-1}$$

To evaluate Eq. (A-1), we calculate $E[\tilde{s}_{1,2}(t)]$, $E[\{\tilde{s}_{1,2}(t)\}^2]$, and $E[\tilde{s}_1(t)\tilde{s}_2(t)]$. First, the mean $E[\tilde{s}_i(t)]$ $(i = 1, 2)$ can be calculated as

$$
\begin{aligned}
E[\tilde{s}_i] &= \text{prob.}(s_i \geq h) \cdot 1 + \text{prob.}(s_i < h) \cdot (-1) \\
&= \text{prob.}(\xi + \eta_i \geq h) - \text{prob.}(\xi + \eta_i < h) \\
&= \int \text{prob.}(\xi + \eta_i \geq h \mid \xi) p_\xi(\xi) d\xi - \int \text{prob.}(\xi + \eta_i < h \mid \xi) p_\xi(\xi) d\xi \\
&= \int \text{prob.}(\eta_i \geq h - \xi \mid \xi) p_\xi(\xi) d\xi - \int \text{prob.}(\eta_i < h - \xi \mid \xi) p_\xi(\xi) d\xi \\
&= \int \{1 - \Phi_\eta(h - \xi)\} p_\xi(\xi) d\xi - \int \Phi_\eta(h - \xi) p_\xi(\xi) d\xi = 1 - 2 \int \Phi_\eta(h - \xi) p_\xi(\xi) d\xi, \quad \text{(A-2)}
\end{aligned}
$$

where prob.$(\cdot \mid \xi)$ indicates conditional probability with fixed ξ. Meanwhile, $E[\tilde{s}_1(t)\tilde{s}_2(t)]$ in the numerator can be expressed as

$$
\begin{aligned}
E[\tilde{s}_1 \tilde{s}_2] = &\ \text{prob.}(s_1 \geq h, s_2 \geq h) \cdot 1 \cdot 1 \\
&+ \text{prob.}(s_1 \geq h, s_2 < h) \cdot 1 \cdot (-1) \\
&+ \text{prob.}(s_1 < h, s_2 \geq h) \cdot (-1) \cdot 1 \\
&+ \text{prob.}(s_1 < -h, s_2 < h) \cdot (-1) \cdot (-1). \quad \text{(A-3)}
\end{aligned}
$$

The first term can be calculated as

$$
\begin{aligned}
&\text{prob.}(s_1 = \xi + \eta_1 \geq h,\ s_2 = \xi + \eta_2 \geq h) \\
&= \int \text{prob.}(\xi + \eta_1 \geq h,\ \xi + \eta_2 \geq h \mid \xi)\ p_\xi(\xi)\ d\xi \\
&= \int \text{prob.}(\xi + \eta_1 \geq h \mid \xi)\ \text{prob.}(\xi + \eta_2 \geq h \mid \xi)\ p_\xi(\xi)\ d\xi \\
&= \int \text{prob.}(\eta_1 \geq h - \xi \mid \xi)\ \text{prob.}(\eta_2 \geq h - \xi \mid \xi)\ p_\xi(\xi)\ d\xi \\
&= \int \{1 - \Phi_\eta(h - \xi)\}^2\ p_\xi(\xi)\ d\xi, \quad \text{(A-4)}
\end{aligned}
$$

where the relation

$$
\text{prob.}(\eta_{1,2} \geq h - \xi \mid \xi) = 1 - \text{prob.}(\eta_{1,2} \leq h - \xi \mid \xi) = 1 - \Phi_\eta(h - \xi) \quad \text{(A-5)}
$$

is used. The other terms can also be calculated as

$$
\begin{aligned}
&\text{prob.}(s_1 = \xi + \eta_1 \geq h, s_2 = \xi + \eta_2 < h) \\
&= \int \text{prob.}(\eta_1 \geq h - \xi \mid \xi)\ \text{prob.}(\eta_2 < h - \xi \mid \xi)\ p_\xi(\xi)\ d\xi \\
&= \int \{1 - \Phi_\eta(h - \xi)\} \Phi_\eta(h - \xi)\ p_\xi(\xi)\ d\xi, \quad \text{(A-6)}
\end{aligned}
$$

$$
\begin{aligned}
&\text{prob.}(s_1 = \xi + \eta_1 < h, s_2 = \xi + \eta_2 \geq h) \\
&= \int \text{prob.}(\eta_1 < h - \xi \mid \xi)\ \text{prob.}(\eta_2 \geq h - \xi \mid \xi)\ p_\xi(\xi)\ d\xi \\
&= \int \Phi_\eta(h - \xi) \{1 - \Phi_\eta(h - \xi)\}\ p_\xi(\xi)\ d\xi, \quad \text{(A-7)}
\end{aligned}
$$

and

$$
\begin{aligned}
&\text{prob.}(s_1 = \xi + \eta_1 < h,\ s_2 = \xi + \eta_2 < h) \\
&= \int \text{prob.}(\eta_1 < h - \xi \mid \xi)\ \text{prob.}(\eta_2 < h - \xi \mid \xi)\ p_\xi(\xi)\ d\xi \\
&= \int \Phi_\eta(h - \xi)^2\ p_\xi(\xi)\ d\xi, \quad \text{(A-8)}
\end{aligned}
$$

which yields

$$E[\tilde{s}_1\tilde{s}_2] = \int \{1 - 2\Phi_\eta(h-\xi)\}^2 p_\xi(\xi)d\xi. \tag{A-9}$$

Similarly, $E[\{\tilde{s}_{1,2}\}^2]$ in the denominator can be calculated as

$$E[\tilde{s}_i^2] = \text{prob.}(s_i \geq h)\cdot 1^2 + \text{prob.}(s_i < h)\cdot(-1)^2 = 1 \tag{A-10}$$

for $i = 1, 2$. Plugging Eqs. (A-2), (A-9), and (A-10) into Eq. (A-1), we obtain Eq. (8).

B. Derivation of Eqs. (9) and (10)

Here, we derive the approximate expressions of $\tilde{\rho}$ in Eqs. (9) and (10). For this purpose, we show that the following approximation hold:

$$\int_{-\infty}^{\infty} \Phi_\eta(u-h)p_\xi(u)du = 1 - \Phi_\xi(h) + O\left(\Phi''_\xi(h)\sigma_\eta^2\right), \tag{B-1}$$

$$\int_{-\infty}^{\infty} \Phi_\eta^2(u-h)p_\xi(u)du = 1 - \Phi_\xi(h) - p_\xi(h)\int_{-\infty}^{\infty}\Phi_\eta(u)\{1-\Phi_\eta(u)\}du + O\left(\Phi''_\xi(h)\sigma_\eta^2\right). \tag{B-2}$$

We first derive Eq. (B-1). By partial integration, the left-hand side can be transformed as

$$\int_{-\infty}^{\infty} \Phi_\eta(u-h)p_\xi(u)du = 1 - \int_{-\infty}^{\infty} p_\eta(u-h)\Phi_\xi(u)du, \tag{B-3}$$

where $\Phi_\xi(u)$ is a CDF of $p_\xi(u)$. Expanding $\Phi_\xi(u)$ in a Taylor series around $u = h$ and ignoring the second and higher-order terms, we can rewrite the right-hand side of Eq. (B-3) as

$$\begin{aligned}
&1 - \int_{-\infty}^{\infty} p_\eta(u-h)\left\{\Phi_\xi(h) + \Phi'_\xi(h)(u-h) + O\left(\Phi''_\xi(h)(u-h)^2\right)\right\}du \\
&= 1 - \Phi_\xi(h)\int_{-\infty}^{\infty} p_\eta(u-h)du - \Phi'_\xi(h)\int_{-\infty}^{\infty}(u-h)p_\eta(u-h)du \\
&\quad + O\left(\Phi''_\xi(h)\int_{-\infty}^{\infty}(u-h)^2 p_\eta(u-h)du\right) = 1 - \Phi_\xi(h) + O\left[\left(\Phi''_\xi(h)\sigma_\eta^2\right)\right],
\end{aligned} \tag{B-4}$$

where we used the assumption that the independent noise is zero mean. We next derive Eq. (B-2). By partial integration, the left-hand side can be transformed as

$$\int_{-\infty}^{\infty} \Phi_\eta^2(u-h)p_\xi(u)du = 1 - 2\int_{-\infty}^{\infty} p_\eta(u-h)\Phi_\eta(u-h)\Phi_\xi(u)du. \tag{B-5}$$

By expanding $\Phi_\xi(u)$ in a Taylor series around $u = h$ and ignoring the second and higher-order terms, we can rewrite the right-hand side of Eq. (B-5) as

$$\begin{aligned}
&1 - 2\int_{-\infty}^{\infty} p_\eta(u-h)\Phi_\eta(u-h)\left\{\Phi_\xi(h) + \Phi'_\xi(h)(u-h) + O\left(\Phi''_\xi(h)(u-h)^2\right)\right\}du \\
&= 1 - 2\Phi_\xi(h)\int_{-\infty}^{\infty} p_\eta(u-h)\Phi_\eta(u-h)du - 2\Phi'_\xi(h)\int_{-\infty}^{\infty}(u-h)p_\eta(u-h)\Phi_\eta(u-h)du \\
&\quad + O\left[\Phi''_\xi(h)\int_{-\infty}^{\infty}(u-h)^2 p_\eta(u-h)\Phi_\eta(u-h)du\right].
\end{aligned} \tag{B-6}$$

Here, the integrals in Eq. (B-6) can be performed as

$$\int_{-\infty}^{\infty} p_\eta(u-h)\Phi_\eta(u-h)du = \frac{1}{2}\int_{-\infty}^{\infty}\frac{d}{du}\{\Phi_\eta(u-h)\}^2 du = \frac{1}{2}, \tag{B-7}$$

$$\int_{-\infty}^{\infty}(u-h)p_\eta(u-h)\Phi_\eta(u-h)du=\int_{-\infty}^{\infty}u'p_\eta(u')\Phi_\eta(u')du'$$
$$=\int_{-\infty}^{\infty}u'p_\eta(u')\left\{\Phi_\eta(u')-\frac{1}{2}\right\}du'+\frac{1}{2}\int_{-\infty}^{\infty}u'p_\eta(u')du'$$
$$=\frac{1}{2}\int_{-\infty}^{\infty}u'\frac{d}{du'}[\Phi_\eta(u')\{\Phi_\eta(u')-1\}]du'=\frac{1}{2}\int_{-\infty}^{\infty}\Phi_\eta(u')\{1-\Phi_\eta(u')\}du', \tag{B-8}$$

and

$$O\left[\Phi''_\xi(h)\int_{-\infty}^{\infty}(u-h)^2p_\eta(u-h)\Phi_\eta(u-h)du\right]$$
$$=O\left[\Phi''_\xi(h)\int_{-\infty}^{\infty}(u-h)^2p_\eta(u-h)\{\Phi_\eta(h)+O[(u-h)]\}\right]du=O\left(\Phi''_\xi(h)\sigma_\eta^2\right), \tag{B-9}$$

where we again used the assumption that the independent noise is zero mean. Thus, plugging Eqs. (B-7), (B-8) into Eq. (B-6), we can derive the approximation in Eq. (B-2), and Eq. (9) follows from Eqs. (B-1) and (B-2). Furthermore, when the independent noise is Gaussian, the following integral formula holds:

$$\int_{-\infty}^{\infty}\Phi_\eta(u)\{1-\Phi_\eta(u)\}du=\frac{\sigma_\eta}{\sqrt{\pi}}. \tag{B-10}$$

Plugging this result into Eq. (9), we obtain Eq. (10).

C. Numerical generation of noisy signals

From given uncorrelated time sequences $f_i(t')$ $(t'=1,2,3,\ldots,N,\ i=1,2)$ satisfying $E[(f_i(k)-E[f_i(k)])(f_j(l)-E[f_j(l)])]=0$ $(i\neq j$ or $k\neq l)$, we define the noisy signals $s_i(t)$ as follows:

$$s_i(t)=\sum_{j=1}^{N}f_i(j)\{U(t-(j-1)\delta t)-U(t-j\delta t)\} \tag{C-1}$$

where $U(t)$ is a Heaviside step function satisfying $U(t)=0$ $(t<0)$, 1 $(t\geq 0)$, and δt determines the time unit of the noisy signal. We use $\delta t=0.1$ in the numerical simulations. In this case, the noisy signal $s_i(t)$ has the following autocorrelation function $C_i(t)$:

$$C_i(t)=E\left[\left(f_i(t')-E[f_i(t')]\right)^2\right]\left(1-\frac{|t|}{\delta t}\right)\quad(-\delta t<t<\delta t),\quad 0\quad\text{(otherwise)}. \tag{C-2}$$

The power spectrum $P_i(\Omega)$ is given by

$$P_i(\Omega)=\int_{-\infty}^{\infty}C_i(t)e^{-i\Omega t}dt=E\left[\left(f_i(t')-E[f_i(t')]\right)^2\right]\frac{2-2\cos(\Omega\delta t)}{\Omega^2\delta t}. \tag{C-3}$$

D. Gaussian case

From the numerical results, it is conjectured that the threshold filter does not enhance the noise correlation if both common and independent noise terms are Gaussian. It is difficult to prove this conjecture rigorously from the general expression of the filtered correlation $\tilde{\rho}$, Eq. (8), but, in the limit of weak independent noise, we can show that this conjecture actually holds true by using the approximate expression for $\tilde{\rho}$, Eq. (10), which is valid when $\sigma_\eta\ll\sigma_\xi$, i.e., in the physical situation that we typically assume. Let us denote the PDF of the Gaussian common noise as

$$p_\xi(u)=\frac{1}{\sqrt{2\pi}\sigma_\xi}\exp\left(-\frac{u^2}{2\sigma_\xi^2}\right)=\frac{1}{\sigma_\xi}p\left(\frac{u}{\sigma_\xi}\right), \tag{D-1}$$

where $y=u/\sigma_\xi$ and $p(y)$ denotes a normal distribution,

$$p(y)=\frac{1}{\sqrt{2\pi}}\exp\left(-\frac{y^2}{2}\right). \tag{D-2}$$

The CDF of the common noise ξ is given by

$$\Phi_\xi(u) = \int_{-\infty}^{u} p_\xi(u')du' = \int_{-\infty}^{u/\sigma_\xi} p(y)dy = \Phi\left(\frac{u}{\sigma_\xi}\right), \tag{D-3}$$

where

$$\Phi(y) = \int_{-\infty}^{y} p(y)dy. \tag{D-4}$$

As shown in Fig. 3, the optimal threshold value appears to be $h = 0$ when both noise terms are Gaussian. This can be shown as follows for the approximate filtered correlation $\tilde{\rho}$. Since Eq. (10) can be transformed as

$$\tilde{\rho} = 1 - \frac{\sigma_\eta p_\xi(h)}{\sqrt{\pi}\Phi_\xi(h)(1-\Phi_\xi(h))} + O\left[\left(\frac{\sigma_\eta}{\sigma_\xi}\right)^2\right] = 1 - \frac{1}{\sqrt{\pi}}\frac{\sigma_\eta}{\sigma_\xi}\frac{p(z)}{\Phi(z)(1-\Phi(z))} + O\left[\left(\frac{\sigma_\eta}{\sigma_\xi}\right)^2\right], \tag{D-5}$$

where $z = h/\sigma_\xi$, $\tilde{\rho}$ depends on h only through $z = h/\sigma_\xi$. As shown in Fig. D-1(a), the function

$$f(z) = \frac{p(z)}{\Phi(z)(1-\Phi(z))} \tag{D-6}$$

in the right-hand side of Eq. (D-5) takes a minimum value $2\sqrt{2}/\sqrt{\pi}$ at $z = 0$, where we used $p(0) = 1/\sqrt{2\pi}$ and $\Phi(0) = 1/2$. Therefore, $\tilde{\rho}$ takes its maximum value

$$\tilde{\rho}_{max} = 1 - \frac{1}{\sqrt{\pi}}\frac{\sigma_\eta}{\sigma_\xi}\frac{p(0)}{\Phi(0)(1-\Phi(0))} + O\left[\left(\frac{\sigma_\eta}{\sigma_\xi}\right)^2\right] = 1 - \frac{2\sqrt{2}}{\pi}\frac{\sigma_\eta}{\sigma_\xi} + O\left[\left(\frac{\sigma_\eta}{\sigma_\xi}\right)^2\right] \tag{D-7}$$

at $z = h = 0$ irrespective of the value σ_ξ. Comparing this maximum filtered correlation with the raw correlation in Eq. (6),

$$\rho = \frac{\sigma_\xi^2}{\sigma_\xi^2 + \sigma_\eta^2} = \frac{1}{1 + \left(\frac{\sigma_\eta}{\sigma_\xi}\right)^2} = 1 - \left(\frac{\sigma_\eta}{\sigma_\xi}\right)^2 + O\left[\left(\frac{\sigma_\eta}{\sigma_\xi}\right)^4\right], \tag{D-8}$$

it is obvious that $\tilde{\rho}_{max} < \rho$ as long as $0 < \sigma_\eta \ll \sigma_\xi$, because $\tilde{\rho}_{max}$ decreases linearly with σ_η/σ_ξ while ρ decreases quadratically, as shown in Fig. D-1(b). Thus, the threshold filter cannot enhance the noise correlation when both common and independent noise terms are Gaussian and the independent noise is sufficiently weaker than the common noise.

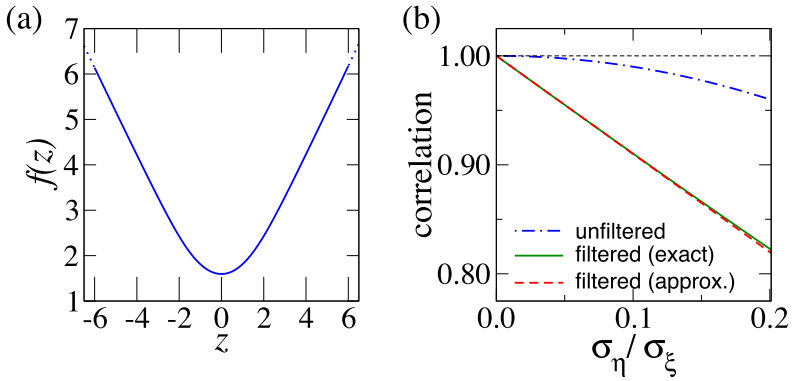

Fig. D-1. (a) Function $f(z)$. (b) Raw correlation ρ and the maximum of the approximate filtered correlation $\tilde{\rho}_{max}$. Exact filtered correlation $\tilde{\rho}$ with $\sigma_\xi = 1$ and $h = 0$ is also shown for comparison.

E. Difference in the distribution of the independent noise

In our theoretical analysis, we assumed that the independent noise terms $\eta_1(t)$ and $\eta_2(t)$ obey the same distribution $p_\eta(\eta)$ for simplicity. This is also because we typically consider the case that the two correlated noisy signals are measured in physically similar situations, e.g. by two signal sensors placed nearby, and thus the independent noisy signals superimposed on the common signal have similar statistics. Actually, the quality of the noise-induced synchronization is essentially determined by the common noise and the distributions of the independent noise terms are not so relevant as long as they are weak and unbiased. To illustrate this, we here show an example of noise-induced synchronization of two oscillators driven by

$$s_1(t) = \xi(t) + \eta_1(t), \quad s_2(t) = \xi(t) + \eta_2(t), \tag{E-1}$$

where $\eta_1(t)$ and $\eta_2(t)$ obey two different distributions chosen from a Gaussian distribution $p_1(\eta)$, a triangular distribution $p_2(\eta)$ and a Laplace distribution $p_3(\eta)$,

$$p_1(\eta) = \frac{1}{\sqrt{2\pi}\sigma_\eta} \exp\left[-\frac{\eta^2}{2\sigma_\eta^2}\right], \quad p_2(\eta) = \frac{1}{\sqrt{2}\sigma_\eta} \exp\left[-\frac{\sqrt{2}|\eta|}{\sigma_\eta}\right],$$
$$p_3(\eta) = \frac{\sqrt{6}\sigma_\eta - |\eta|}{6\sigma_\eta^2} \quad (-\sqrt{6}\sigma_\eta \le \eta \le \sqrt{6}\sigma_\eta), \quad 0 \quad \text{(otherwise)}. \tag{E-2}$$

We assume that both $\eta_1(t)$ and $\eta_2(t)$ are zero-mean and possess the same standard deviation $\sigma_\eta = 0.3$, and the common noise obeys the quodratic bimodal distribution in Fig. 2(d). The natural frequency of the oscillators is fixed at $\omega = 1$, and the phase sensitivity function of both oscillators is $Z(\theta) = 0.1 \sin\theta$.

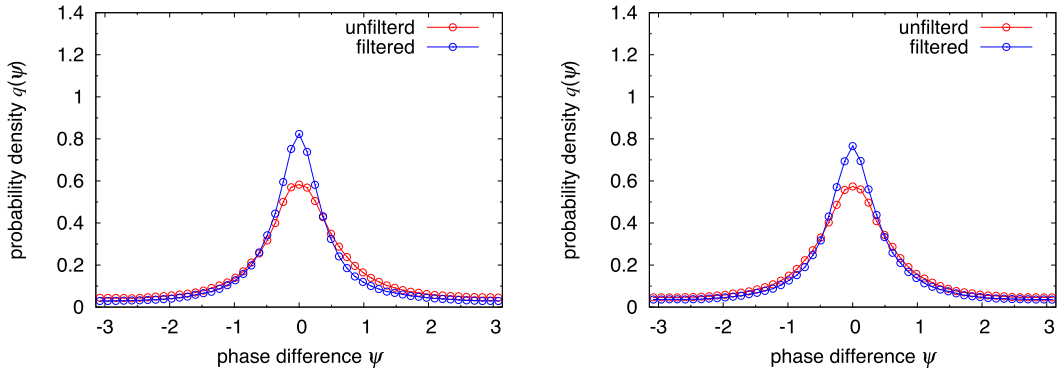

(a) η_1: Gaussian, η_2: Triangular

(b) η_1: Gaussian, η_2: Laplace

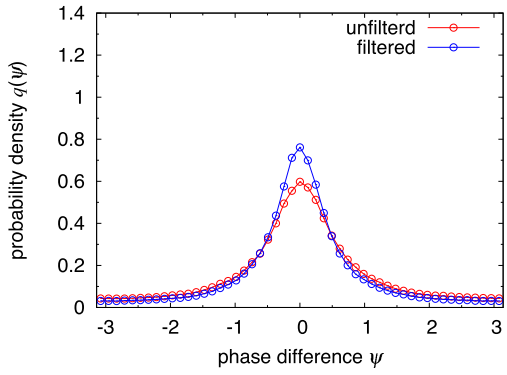

(c) η_1: Triangular, η_2: Laplace

Fig. E-1. Stationary probability density functions of the phase difference between two oscillators driven by correlated noisy signals, where the independent noisy signals obey different statistics. Red curves are obtained for raw noisy signals without filtering, and blue curves show the results for filtered noisy signals. (a) $\rho = 0.87$, $\tilde{\rho} = 0.93$, $R_1 = 0.45$, $\tilde{R}_1 = 0.68$, (b) $\rho = 0.87$, $\tilde{\rho} = 0.92$, $R_1 = 0.42$, $\tilde{R}_1 = 0.65$, (c) $\rho = 0.87$, $\tilde{\rho} = 0.93$, $R_1 = 0.43$, $\tilde{R}_1 = 0.67$.

Figure E-1 shows the PDFs of the stationary phase difference between the two oscillators driven by s_1 and s_2, which are obtained by direct numerical simulations. It can be seen that the threshold filter actually improve noise-induced synchronization between the oscillators even if the independent noise terms obey different statistics.

References

[1] Z.F. Mainen and T.J. Sejnowski, "Reliability of spike timing in neocortical neurons," *Science*, vol. 268, no. 5216, pp. 1503–1506, 1995.

[2] A. Uchida, R. McAllister, and R. Roy, "Consistency of nonlinear system response to complex drive signals," *Phys. Rev. Lett.*, vol. 93, no. 24, 244102, 2004.

[3] K. Yoshida, K. Sato, and A. Sugamata, "Noise-induced synchronization of uncoupled nonlinear systems," *J. Sound Vib.*, vol. 290, no. 1–2, pp. 34–47, 2006.

[4] R.F. Galán, N. Fourcaud-Trocmé, G.B. Ermentrout, and N.N. Urban, "Correlation-Induced Synchronization of Oscillations in Olfactory Bulb Neurons," *J. Neurosci.*, vol. 26, no. 14, pp. 3646–3655, 2006.

[5] M.D. Binder and R.K. Powers, "Relationship Between Simulated Common Synaptic Input and Discharge Synchrony in Cat Spinal Motoneurons," *J. Neurophysiol.*, vol. 86, no. 5, 2266–2275, 2001.

[6] P.A.P. Moran, "The statistical analysis of the Canadian Lynx cycle," *Aust. J. Zool.*, vol. 1, no. 3, pp. 291–298, 1953.

[7] K. Nakada, S. Yakata, and T. Kimura, "Noise-induced synchronization in spin torque nano oscillators," *J. Appl. Phys.*, vol. 111, no. 7, 07C920, 2012.

[8] M. Harashima, H. Yasuda, and M. Hasegawa, "Synchronization of wireless sensor networks using natural environmental signals based on noise-induced phase synchronization phenomenon," *2012 IEEE Vehicular Technology Conference*, Yokohama, May 6–9, 2012.

[9] J.-N. Teramae and D. Tanaka, "Robustness of the noise-induced phase synchronization in a general class of limit cycle oscillators," *Phys. Rev. Lett*, vol. 93, no. 20, 204103, 2004.

[10] D.S. Goldobin and A.S. Pikovsky, "Synchronization of self-sustained oscillators by common white noise," *Physica A*, vol. 351, no. 1, pp. 126–132, 2005.

[11] Y. Kuramoto, *Chemical Oscillations, Waves and Turbulence*, Dover, New York, 2003.

[12] D.S. Goldobin, J.-N. Teramae, H. Nakao, and G.B. Ermentrout, "Dynamics of limit-cycle oscillators subject to general noise," *Phys. Rev. Lett.*, vol. 105, no. 15, 154101, 2010.

[13] H. Nakao, K. Arai, and Y. Kawamura, "Noise-induced synchronization and clustering in ensembles of uncoupled limit-cycle oscillators," *Phys. Rev. Lett.*, vol. 98, no. 18, 184101, 2007.

[14] W. Kurebayashi, K. Fujiwara, and T. Ikeguchi, "Colored noise induces synchronization of limit cycle oscillators," *Europhys. Lett.*, vol. 97, no. 5, 50009, 2012.

[15] P. Zhou, S.D. Burton, N.N. Urban, and G.B. Ermentrout, "Impact of neuronal heterogeneity on correlated colored noise-induced synchronization", *Front. Comput. Neurosci.*, vol. 7, no. 113, doi:10.3389/fncom.2013.00113, 2013.